Artificial Intelligence for Engineering Design, Analysis and Manufacturing (2011), *25*, 357–374.

doi:10.1017/S0890060411000217

A coupled configurational description of boundary shape based on distance and directionality

ERMAL SHPUZA
Southern Polytechnic State University, Marietta, Georgia, USA
(Received October 29, 2010; Accepted February 7, 2011)

Abstract

A configurational method for describing shape is proposed based on two measures that gauge human experiences of moving through space: distance and changes in direction of travel. Boundary shapes from the built environment and nature are studied in a morphospace composed of two axes: one corresponding to each measure, to yield a typological classification of form. It is shown that the covariance between distance and directionality is mediated by the topological structure of embedded main circulation. Three kinds of circulation—elementary, ring, and linear—thus affect three fundamentally different balancing conditions between distance and directionality in boundary shapes. The analysis of large samples of shapes thus far demonstrates a "unique shape" status, where no two different shapes have the same pair of relative distance and directional fragmentation values.

Keywords: Configurational; Directional Fragmentation; Relative Distance; Shape; Unique

1. INTRODUCTION

The built environment is considered at two distinct scales: the boundary conditions exemplified by building shells and urbanized territories and the embedded circulation systems of corridors and streets. Analytical models that consider interrelations between the two scales are especially important for the study of building types where the two have different life spans. For example, although office layouts are modified frequently due to changes in organizational models, their design and planning take into consideration the constraining effect of the permanent building shells (Duffy, 1974). Exhibition curators face similar issues, reconciling the ever-changing layout strategies and artifact contents with the permanent shells of museums and art galleries (Zamani, 2008). Such interrelations are also worth studying because boundary conditions and circulations systems are influenced by specific factors of distinct origin. Although building shells are affected by structural, environmental, and construction systems, interior layouts take into account factors that range from ergonomics to organizational models.

The effect of boundary on contained spatial systems has been an inquiry within architectural discourse for quite some time. In 1928, Krasil'nikov (Cooke, 1975) proposed a mathematical model to explain the relation between the geometry of floorplate and the travel time from the entrance to workplaces in a building. Floorplate shapes have been shown to affect the distance of travel between internal locations (Willoughby, 1975; Tabor, 1976) and travel distance between day-lit strips in buildings (Steadman, 2003). Floorplate shapes in office buildings have been shown to affect the spatial integration (a measure of directional distance) of layouts (Shpuza & Peponis, 2008). Similarly, urban shapes have been shown to affect the integration of street networks in cities (Shpuza, 2007).

Research in space syntax (Hillier & Hanson, 1989; Hillier, 1996; Peponis & Wineman, 2002) has primarily studied contained space. This configurational approach scrutinizes relational patterns among discrete components of building interiors and public spaces in cities to explain the built environment as a social product. A substantial body of empirical research has demonstrated strong affinities between underlying configurational features of space and various aspects of spatial cognition, behavioral patterns, and social function. Originally, studies in space syntax assessed topological characteristics of space to evaluate its social function; the early work did not consider geometric shape. More recent developments in space syntax theory augment original topological descriptions of space with metrics for shape (Hillier, 1996). Street networks have been conceptualized as independent systems with their own internal logic tied to patterns of street connectivity, which evolve by resolving the paradoxes of centrality and visibility (Hillier, 1996, 1999). Experiments in partitioning grids have

Reprint requests to: Ermal Shpuza, Department of Architecture, Southern Polytechnic State University, 1100 South Marietta Parkway, Marietta, GA 30060, USA. E-mail: ermal@morphostudio.net

illustrated the dependence of grids on topological relations and explained the emergence of the street geometry of deformed grids. However, with the exception of the torus shape (Hillier, 1996), no attention has been given to the mutual effect of the boundary and structural pattern it contains in built environments. For example, the street structures of London and New York reflect not only patterns of the deformed wheel and the Manhattan grid, respectively, but also the cropping effect of Thames, Hudson, and East Rivers.

In summary, the effect of embedded circulation systems on boundary conditions is little understood. This study is aimed at testing the hypothesis that boundary shapes exhibit characteristics that are intrinsically tied to the generative principles underlying the circulation systems they contain, over and above the influences of site context. As a corollary, such features support morphological classifications in the built environment.

This study is aimed at describing boundary conditions in the built environment according to their two-dimensional (2-D) shape. The boundary shape is considered as a diagram of forces (Thompson, 1959) that originate from inside and outside the boundary, and results in a state of fit (Alexander, 1964). In buildings, these forces are exemplified by requirements for space use, accommodation of layouts, daylight, natural ventilation, building systems, structural limitations, and site constraints. In cities, they represent growth pressures, zoning regulations, the constraining effect of terrains, and the cost of travel between locations. For the purpose of this argument, the built environment is considered from the viewpoint of the social function of space (Hillier & Hanson, 1989). Accordingly, the study tackles the understanding of boundary shape according to internal forces related to patterns of movement, co-presence, co-awareness, and encounter, without considering external forces such as the constraining effects of building sites and terrains. Shapes are regarded as byproducts of the potential internal movement, thus making it possible to gauge in turn the mutual interaction between boundary shapes and contained circulation systems.

The floorplate shape, or the 2-D shape of the slab of a particular floor, is defined according to the conventions used in architectural design. Building cores, shafts, stairs, ramps, atria, courtyards, and light wells are not part of floorplate shapes, and when located inside buildings, they constitute holes in its shape. The floorplate is one of the most permanent among building elements and is often tied to the structural integrity of the building. Holes are considered an integral part of a floorplate and remain unchanged as they provide vertical circulation, light, ventilation, and passage of conduits. Because of their permanence, for the purpose of this argument, floorplate shapes are considered only in their actual state and not according to shape hulls (i.e., ignoring holes).

The urban shape, or the 2-D shape of the urbanized territory, is defined according to the contiguity of its built form, disregarding administrative boundaries, and following two rules as follows. First, notwithstanding obvious physiographic barriers, one has reached the urban boundary when traveling outward from the city center one reaches the point where there are no buildings but only undeveloped land in both sides of a road. Second, roads that provide short-cut connections between outlying peripheral fringes are included in the urbanized territory. Holes in the urban shape are defined as areas located inside the urbanized territory unused for buildings, recreation, or industrial production. Examples of shape holes include agricultural land in the fringes of urban shapes; areas unsuitable for building such as rivers, ravines, steep slopes, bays, lagoons, ponds; and man-made features like canals and railroads. The shape hull results from removing the holes from the urban shape. In contrast to buildings, where the floorplate shape remains unchanged over the years, urban shapes are in continuous flux. Urban growth involves two kinds of processes: the outbound extension of urban shapes, and the infilling of shape holes. From the viewpoint of environmental protection, energy, and commuting time, the infill development of urban holes takes priority to the outbound urban extension. Therefore, the study considers the urban environments according to both the actuality of their urban shape and the potentiality of their shape hulls.

The argument is developed in four parts. First, a review of theories and methods of shape description examines applications suitable for the analysis of boundary shapes in the built

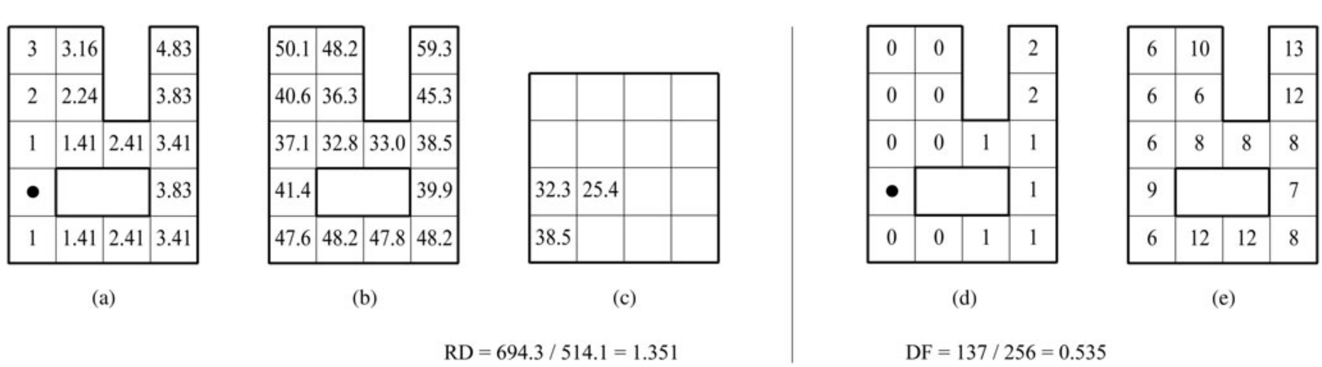

Fig. 1. Measures of shape: (a) short path metric distances from a particular unit in the shape, (b) aggregate distances for all units in the shape, (c) aggregate distances in the equal area square, (d) directional depth from a particular unit in the shape, and (e) aggregate directional depths for all units in the shape.

https://doi.org/10.1017/S0890060411000217 Published online by Cambridge University Press

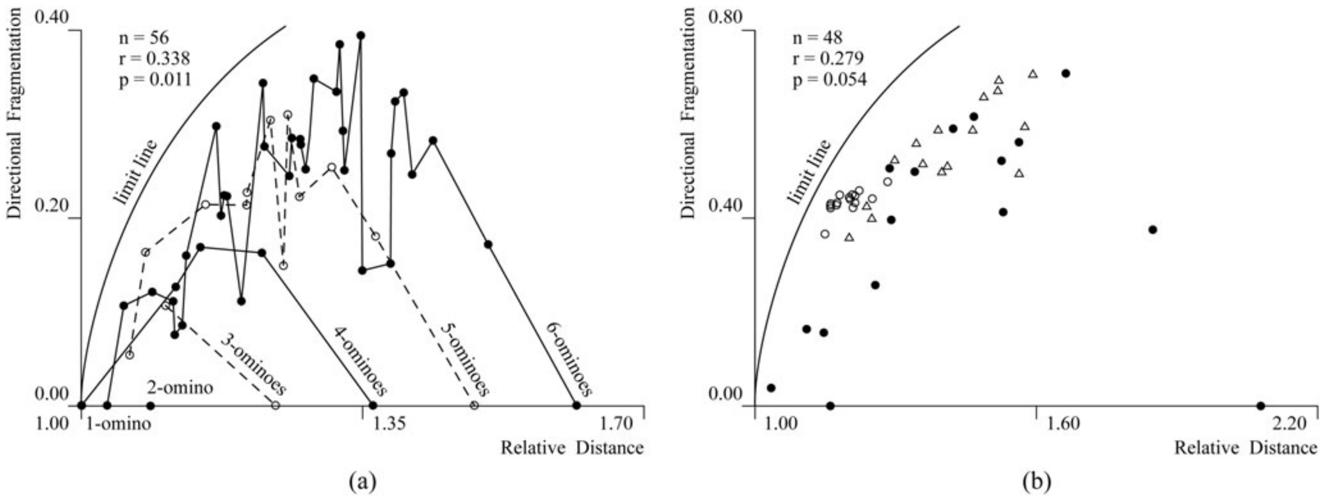

Fig. 2. (a) Series of polyomino shapes ($n = 1$ to 6) in morphospace; (b) scatterplot of sample of 48 decomino shapes including all (○) 16 cases with topological holes, (Δ) 16 cases with nontopological holes, and (•) 16 cases without holes.

environment. Second, two shape descriptions are proposed based on the human experience of moving through space. Third, samples of various classes of boundary shape in the built environment and nature are analyzed according to two measures. Fourth, a discussion addresses the typological classifications of boundaries in the built environment in general and the different states of covariance between two measures according to underlying circulation in particular.

2. METHODS OF SHAPE DESCRIPTION

In the review of methods for describing the compactness of shape, MacEachern (1985) identifies two main approaches for quantifying shape. The first includes methods that address shape uniqueness according to which no shapes that differ from each other can have equal descriptions. These methods employ multiple parameters and complex mathematical models for defining shape. Bunge (1966) proposed a system of unique shape classification based on distances between selected vertices of a polygon. Similarly, the application of dual-axis Fourier analysis to shape analysis (Moellering & Rayner, 1981) suggests a unique description of shape. More recently, the trivariate shape definition (Wentz, 2000) demonstrated that when three indices of edge, elongation, and perforation are used to describe shape, no two different shapes have the same set of numbers.

The second approach includes a vast array of methods that address specific aspects of shape, such as compactness, elongation, and indentation. In general, the indices used by geographers regard various relations among metric distances between shape vertices, perimeter points, and centroids; ratios between actual areas and areas of yardstick shapes; and perimeter (Haggett & Chorley, 1969; March & Steadman, 1971; Austin, 1984; MacEachern, 1985). Compactness is the single most considered aspect that has been formalized in a wide range of indices (Clark & Gaile, 1973; MacEachren, 1985). Shape compactness, measured as the ratio between area and perimeter, has been employed widely by architects as a simple empirical measure for describing building plans (March &

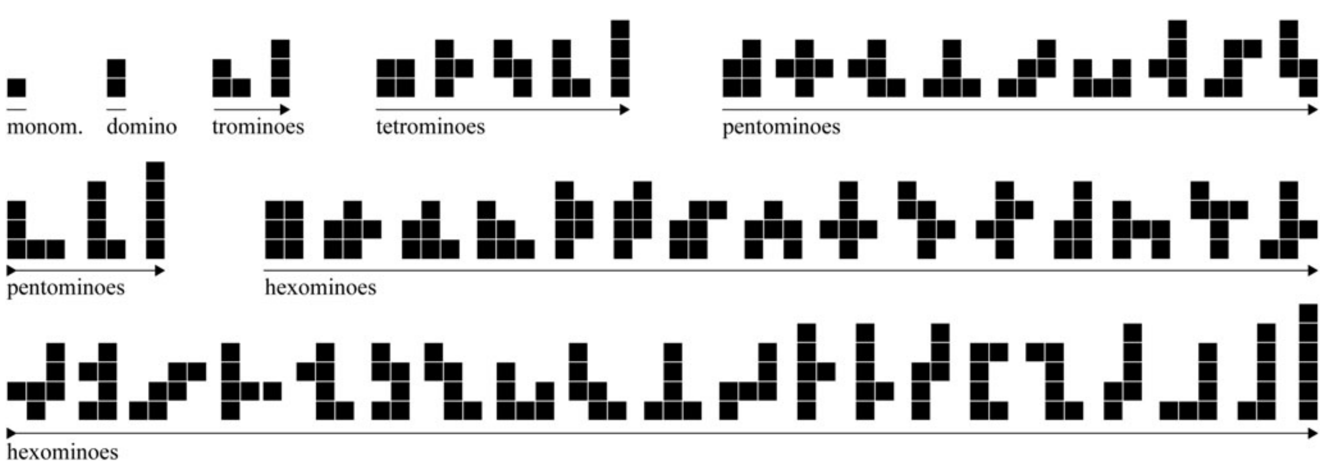

Fig. 3. Polyomino shapes ($n = 1$ to 6) listed according to ascending relative distance values for each group.

https://doi.org/10.1017/S0890060411000217 Published online by Cambridge University Press

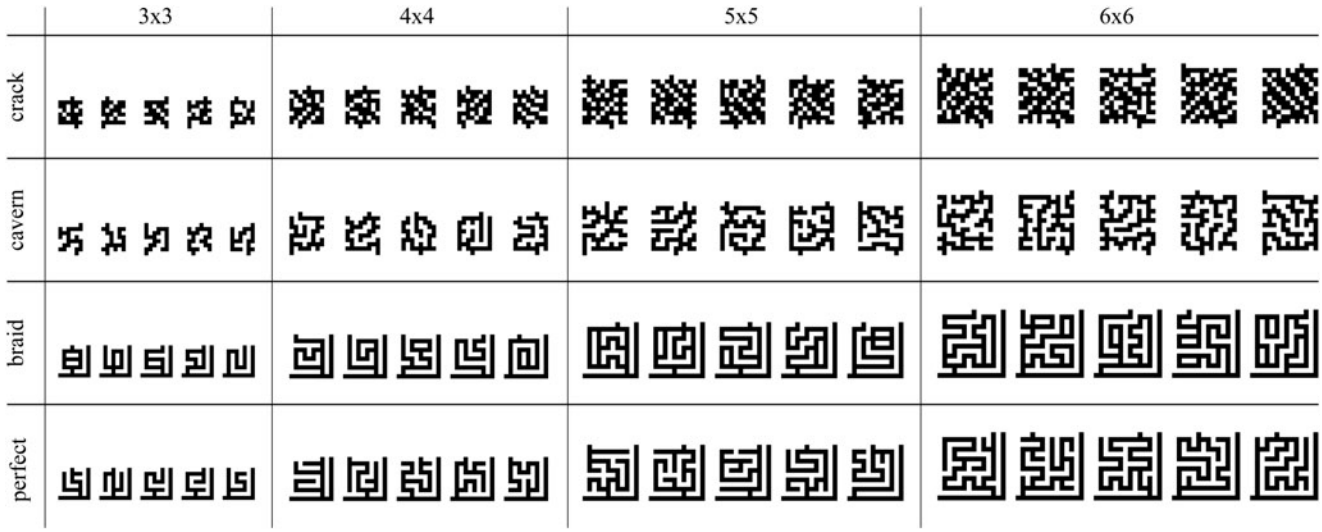

Fig. 4. Mazes generated according to crack, cavern, braid, and perfect algorithms in sizes 3×3, 4×4, 5×5, and 6×6, respectively. Shapes are listed according to ascending relative distance values for each group.

Steadman, 1971). However, this metric has limited accuracy. For example, it can be easily proven that a perimeter jagged in the small scale of local indentations may coincide with a compact shape. Overall, the application of geographical indices based on discrete metric elements for the analysis of the built environment is problematic because discrete elements characterize either local features of shapes or global features that are not related to the human perception of space.

Another class of methods for describing shape is based on infinitesimal representations. A shape is represented with modular units, and specific relations among all units are aggregated into an overall index. According to Blair and Biss (1967), a shape is divided into infinitesimal elements, and distances between all shape units to the center of gravity are aggregated to calculate an index of compactness. It is argued that this method overcomes the problems of dealing with cases of high degree of fragmentation, dispersion into islands, gross distortions, and punctured shapes. Taylor (1971) uses the statistical distribution of metric distances within shapes to gauge the effects of elongality, puncturedness, fragmentation, and indentation.

Only a few methods proposed by research in space syntax address the properties of shape. The descriptions of architectural plans with s-partitions and e-partitions emphasize the importance of shape for determining the definition of elemental convex partitioning (Peponis et al., 1997). The inner spatial structure is considered an effect of bounding shape. Psarra and Grajewski (2001) propose a robust description of space based on the visibility between tessellated units of the enclosing perimeter. However, the indices proposed by these two methods remain unchanged after affinity transformation of shape (parallelism, cross-ratio, and neighborliness) and therefore cannot be used for describing shape.

Recent studies have utilized representations of architectural and urban plans flood-filled with small tessellated units and have proposed spatial descriptions based on patterns of covisibility between the units (Batty, 2001; Conroy, 2001; Turner et al., 2001). Of particular interest to this argument are Turner et al.'s two indices, mean shortest path distance, calculated as the aggregate shortest path metric distance between all modular units, and visual mean depth, calculated as the aggregate of directional changes between all units. However, these methods describe spatial complexes according to properties of specific locations and regions in a spatial complex without compiling any overall shape index.

For the purpose of describing shapes in the built environment, the modular methods have a threefold advantage: first, these methods enable direct associations of representational units with continuous qualities of space, which is essential for describing large unpartitioned boundary spaces. Second, modular representations allow gauging the spatial qualities of the built environment in a configurational manner by con-

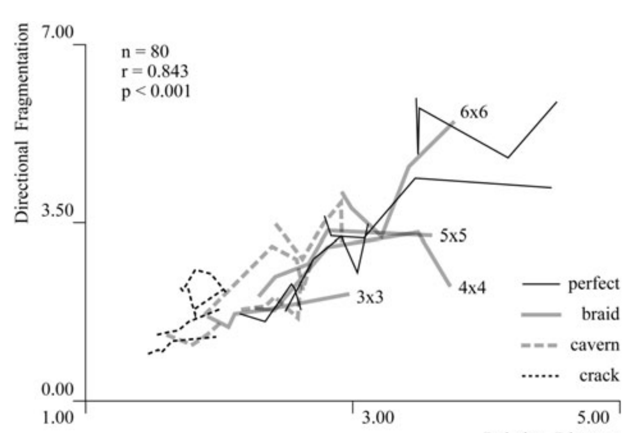

Fig. 5. Morphospace plots of series of crack, cavern, braid, and perfect mazes, generated with 3×3, 4×4, 5×5, and 6×6 sizes, respectively. For clarity, only braid series are labeled.

Table 1. *Catalogue of the sample of 50 houses listed according to ascending relative distance values*

Name	Floor	Architect	Location
1. Malin Residence	U	John Lautner	Los Angeles, CA, USA
2. Casa Rotunda	2	Mario Botta	Stabio, Switzerland
3. Hopkins House	S	M. & P. Hopkins	London, UK
4. Cap Martinet	1	E. Torres, J. Martínez Lapeña	Ibiza, Spain
5. Schröder House	1	Gerrit Rietveld	Utrecht, The Netherlands
6. Furniture House	G	Shigeru Ban	Tamanashi, Japan
7. Esherick House	1	Louis Kahn	Philadelphia, PA, USA
8. Newton Road	1	Denys Lasdun	London, UK
9. House at Santander	1	J. Junquera & E. P. Pita	Santander, Spain
10. Müller House	1	Adolf Loos	Prague, Czech Republic
11. Dickes House	1	Rob Krier	Luxembourg, Luxembourg
12. Wittgenstein House	1	P. Engelmann & L. Wittgenstein	Vienna, Austria
13. Fallingwater	G	Frank Lloyd Wright	Bear Run, PA, USA
14. Farnsworth House	G	Ludwig Mies van der Rohe	Plano, IL, USA
15. Melnikov House	1	Konstantin Melnikov	Moscow, Russia
16. Aluminaire House	1	A. L. Kocher & A. Frey	Syosset, NY, USA
17. Villa Stein-de Monzie	1	Le Corbusier	Paris, France
18. Sun House	G	Edwin Maxwell Fry	London, UK
19. Lovell Health House	1	Richard Neutra	Los Angeles, CA, USA
20. Charlotte House	G	Günter Behnisch	Stuttgart, Germany
21. Wolf House	G	Ludwig Mies van der Rohe	Gubin, Poland
22. San Cristobal	G	Luis Barragán	Mexico City, Mexico
23. Vanna Venturi House	G	Robert Venturi	Philadelphia, PA, USA
24. Maisons Jaoul House A	1	Le Corbusier	Paris, France
25. Rose Seidler House	G	Harry Seidler	Turramurra, NSW, Australia
26. Aluminium House	G	Toyo Ito	Setagaya-ku, Tokyo, Japan
27. Tugendhat House	1	Ludwig Mies van der Rohe	Brno, Czech Republic
28. E1027	1	Eileen Gray	Cap Martin, France
29. Fisher House	G	Louis Kahn	Philadelphia, PA, USA
30. Lange House	1	Ludwig Mies van der Rohe	Krefeld, Germany
31. Villa Savoye	1	Le Corbusier	Poissy, France
32. Bauhaus Staff House	1	Walter Gropius	Dessau, Germany
33. High and Over	1	Amyas Connell	Amersham, UK
34. Robie House	1	Frank Lloyd Wright	Chicago, IL, USA
35. Utzon House	G	Jørn Utzon	Hellebaek, Denmark
36. Villa Ra Roche-Jeanneret East	1	Le Corbusier	Auteuil, France
37. Tallon House	G	Ronnier Tallon	Dublin, Ireland
38. Jacobs House	G	Frank Lloyd Wright	Madison, WI, USA
39. Winston Guest House	G	Frank Gehry	Wayzata, MN, USA
40. Villa Mairea	1	Alvar Aalto	Noormarkku, Finland
41. Case Study House No. 22	G	Pierre Koenig	Los Angeles, CA, USA
42. Villa Girasole	U	Ettore Fagiuoli	Marcellise, Italy
43. Casa Garau Agustí	1	Enric Miralles	Barcelona, Spain
44. Möbius House	G	B. van Berkel & C. Bos	Utrecht, The Netherlands
45. Experimental House	G	Alvar Aalto	Muuratsalo, Finland
46. Creak Vean House	G	N. Foster & R. Rogers	Cornwall, UK
47. Maison Prouvé	G	Jean Prouvé	Nancy, France
48. Schminke House	1	Hans Scharoun	Löbau, Germany
49. House at Moledo	G	E. Souto de Moura	Moledo, Portugal
50. Villa Dall'Ava	1	Rem Koolhaas	Paris, France

sidering relations among all shape units. Third, modular methods take into account dimensional aspects of shape and thus allow weighing the configurational analysis with metrics of size and distance.

From the viewpoint of understanding the effect of circulation systems on boundary shapes, configurational methods can be used to formulate descriptions that are compatible with configurational descriptions of circulation systems in buildings and cities. Movement has been recognized as a basic premise for understanding the built environment (Piaget & Inhelder, 1967; Gibson, 1979). Two measures of shape based on the human experience of moving through space, previously developed by Shpuza (2001) and Shpuza and Peponis (2008), are enhanced for the purpose of this study.

https://doi.org/10.1017/S0890060411000217 Published online by Cambridge University Press

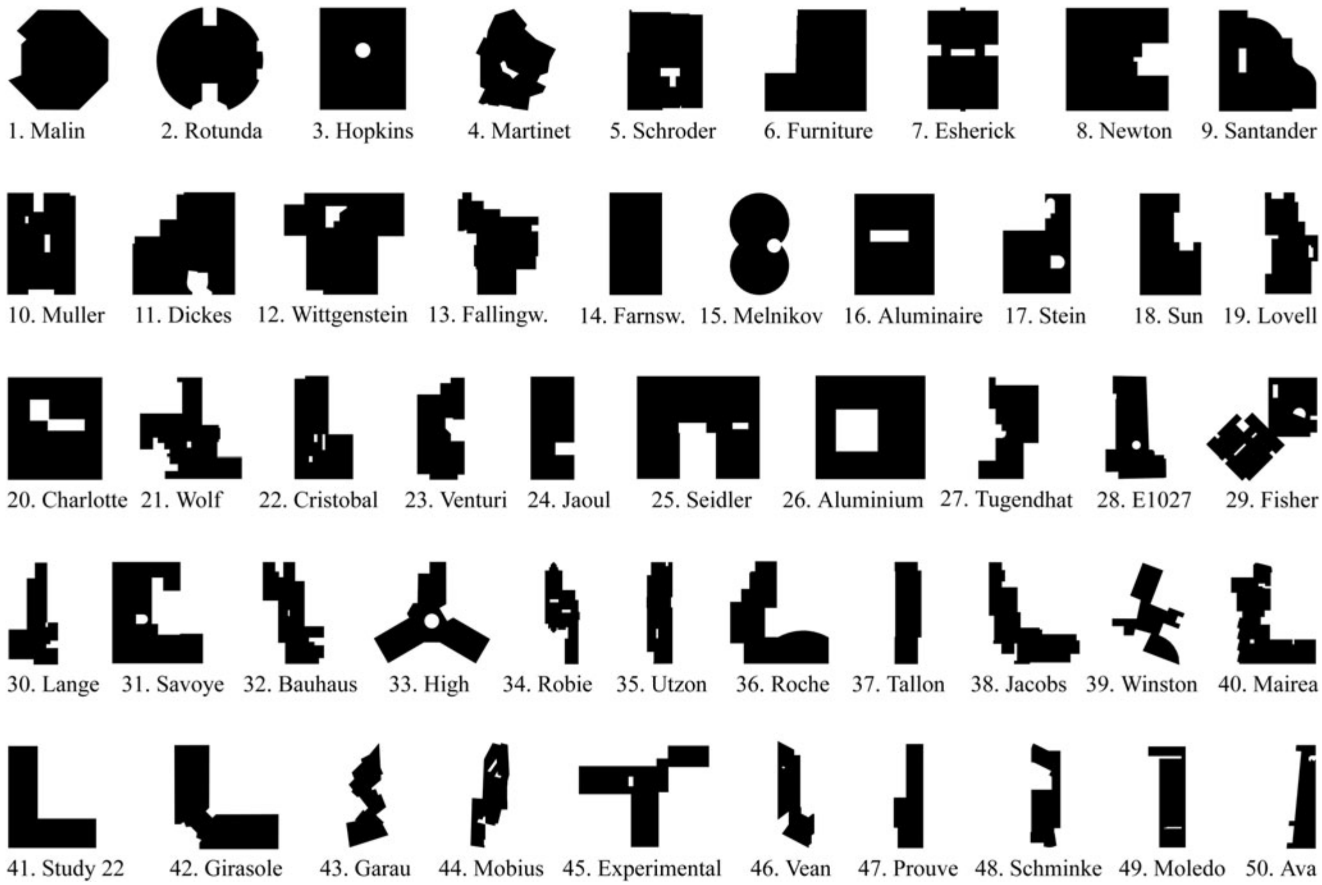

Fig. 6. The sample of 50 house floorplates listed according to ascending relative distance values.

3. RELATIVE DISTANCE (RD)

The first measure, RD, is an index of universal metric distance. It corresponds to the potential energy needed to cover distances between locations inside a shape. In contrast to analytical models that consider distance as an effect of shape, here, distances between points are used to characterize a shape. Shape is considered according to the *structure of the field* and as a *derived entity* of space (Koenderink, 1990) whereby distance is used to define a particular aspect of shape according to an inside to outside approach. A shape is represented with modular square units, and shortest path inner shape distances are computed between pairs of units. The overall distance D for a shape is the sum of aggregated shortest path distances.

$$D = \sum_{i=1,j=1}^{i=n,j=n} d_{ij}, \tag{1}$$

where d_{ij} is the shortest path distance between two units i and j, and n is the number of units in a shape (Fig. 1).

The measure of RD is expressed as the overall distance for the entire shape D normalized by the overall distance in an equal area square D_{eas} (Fig. 1c).

$$\mathrm{RD} = \frac{D}{D_{\mathrm{eas}}}. \tag{2}$$

Because shapes are not always represented with a number of units equal to a square, D_{eas} is obtained by the linear interpolation between distances of the two closest square shapes $D^{\square}$. For example, for a shape represented with 110 units, D_{eas} equals 66,690 after the interpolation between $D^{\square}(100) = 51{,}615$ and $D^{\square}(121) = 83{,}272$. The value of RD for a square therefore equals 1, whereas for a circle it equals 0.980. The RD increases as shapes become elongated or fragmented into wings or by holes.

For the square shape, when taxicab distance δ is used, the overall distance $\Delta^{\square}$ is a function of the number of units used for representing the square (Shpuza, 2006; Shpuza & Peponis, 2008). In contrast, when shortest path distance is used, the overall distance $D^{\square}$ follows a fuzzy logic and cannot be expressed as a function of representation units. However, in a square mapped with 4 units, the ratio $\Delta^{\square}/D^{\square}$ equals 1.172, for a square with 16 units it equals 1.245, whereas for fine representations of more

Table 2. *Catalogue of the sample of 50 office floor plates with ring circulation listed according to ascending relative distance values*

Name	Floor	Architect	Location
1. BT, The Square	T	Arup Assoc.	London, UK
2. MGIC	T	SOM	Milwaukee, WI, USA
3. Direct. of Telec., MPBW	T	Whitehall Dev. Group	Kew, UK
4. Hoffmann–La Roche	T	The Hillier Group	Nutley, NJ, USA
5. RAC Regional	2	N. Grimshaw & Partners	Bristol, UK
6. McDonald's Finland	T	Heikkinen-Komonen	Helsinki, Finland
7. Willis Faber Dumas	1	Norman Foster	Ipswich, UK
8. Look Building	T	Emery Roth & Sons	New York, NY, USA
9. Torre Agbar	T	Ateliers Jean Nouvel	Barcelona, Spain
10. 1 Astor Plaza	T	Kahn & Jacobs, Der Scutt	New York, NY, USA
11. Sears 40th Floor	40	SOM	Chicago, IL, USA
12. 1 Illinois Center	T	Mies van der Rohe	Chicago, IL, USA
13. Fred and Ginger	T	F. Gehry	Prague, Czech Republic
14. 450 Lexington Ave	T	SOM	New York, NY, USA
15. IBM Australia	T	Buchan, Laird & Bawden	Melbourne, Australia
16. 30 St. Mary Axe	21	Foster & Partners	London, UK
17. Proscenium	T	Thompson, Ventulett, Stainbeck	Atlanta, GA, USA
18. Lloyd's	T	Richard Rogers Partnership	London, UK
19. Datapec	3	Kauffmann Theilig	Gniebel, Germany
20. BT, 5 Longwalk	2	Foster & Partners	London, UK
21. Australia Square Tower	T	H. Seidler, P.L. Nervi	Sydney, Australia
22. Citicorp	T	SOM	New York, NY, USA
23. Ark	4	Ralph Erskine	London, UK
24. Apicorp	T	DEGW, Ove Arup & Assoc.	Al Khobar, Saudi Arabia
25. W.R. Grace Building	T	SOM	New York, NY, USA
26. Schömer Haus	T	Heinz Tesar	Klosterneuburg, Austria
27. Aurora Place	41	Renzo Piano Building Workshop	Sydney, Australia
28. Sears 70th Floor	70	SOM	Chicago, IL, USA
29. Imagination	T	Unknown	London, UK
30. Fox Plaza	T	Johnson, Fain & Pereira	Los Angeles, CA, USA
31. 3com Corporation	2	Studios Architecture	Santa Clara, CA, USA
32. Sperry Rand Building, AXA Fi	T	Harrison, Abramovitz, Roth	New York, NY, USA
33. Seagram Building	T	Mies van der Rohe	New York, NY, USA
34. Larkin Building	2	Frank Lloyd Wright	Buffalo, NY, USA
35. Centraal Beheer	3	Herman Hertzberger	Appeldoorn, The Netherlands
36. MetLife Building	T	E. Roth, P. Belluschi, W. Gropius	New York, NY, USA
37. Landstingförbundet	T	Mats Edblöm, L-Konsult	Stockholm, Sweden
38. IBM UK	1	M. Hopkins & Partners	London, UK
39. Genzyme	12	Behnisch	Cambridge, MA, USA
40. Jægergården	T	Nielsen, Nielsen & Nielsen A/S	Århus, Denmark
41. Torre Cube	T	Carme Pinós	Guadalajara, Mexico
42. Unilever	4	Behnisch	Hamburg, Germany
43. BGW	1	LOG ID	Dresden, Germany
44. Gruner + Jahr	2	Steidle Kiessler, Schweger Partn.	Hamburg, Germany
45. SAS	T	Niels Torp	Stockholm, Sweden
46. Olivetti	T	DEGW & Studio De Lucchi	Bari, Italy
47. Credit Bank Peru	4	Arquitectonica	Lima, Peru
48. Norddeutsche Landesbank	8	Behnisch	Hanover, Germany
49. DZ Bank	T	Frank Gehry	Berlin, Germany
50. Federal Environmental Agency	2	Sauerbruch Hutton	Dessau, Germany

than 3000 units, the ratio settles at 1.279.

$$\frac{\Delta^{\square}}{D^{\square}} = 1.279. \qquad (3)$$

Calculations with fine representations of large samples of shape indicate that RD ratios yield almost identical results when computed with taxicab distances and shortest path distances.

$$\frac{D}{D_{\text{eas}}} = \text{RD} \approx R\Delta = \frac{\Delta}{\Delta_{\text{eas}}}. \qquad (4)$$

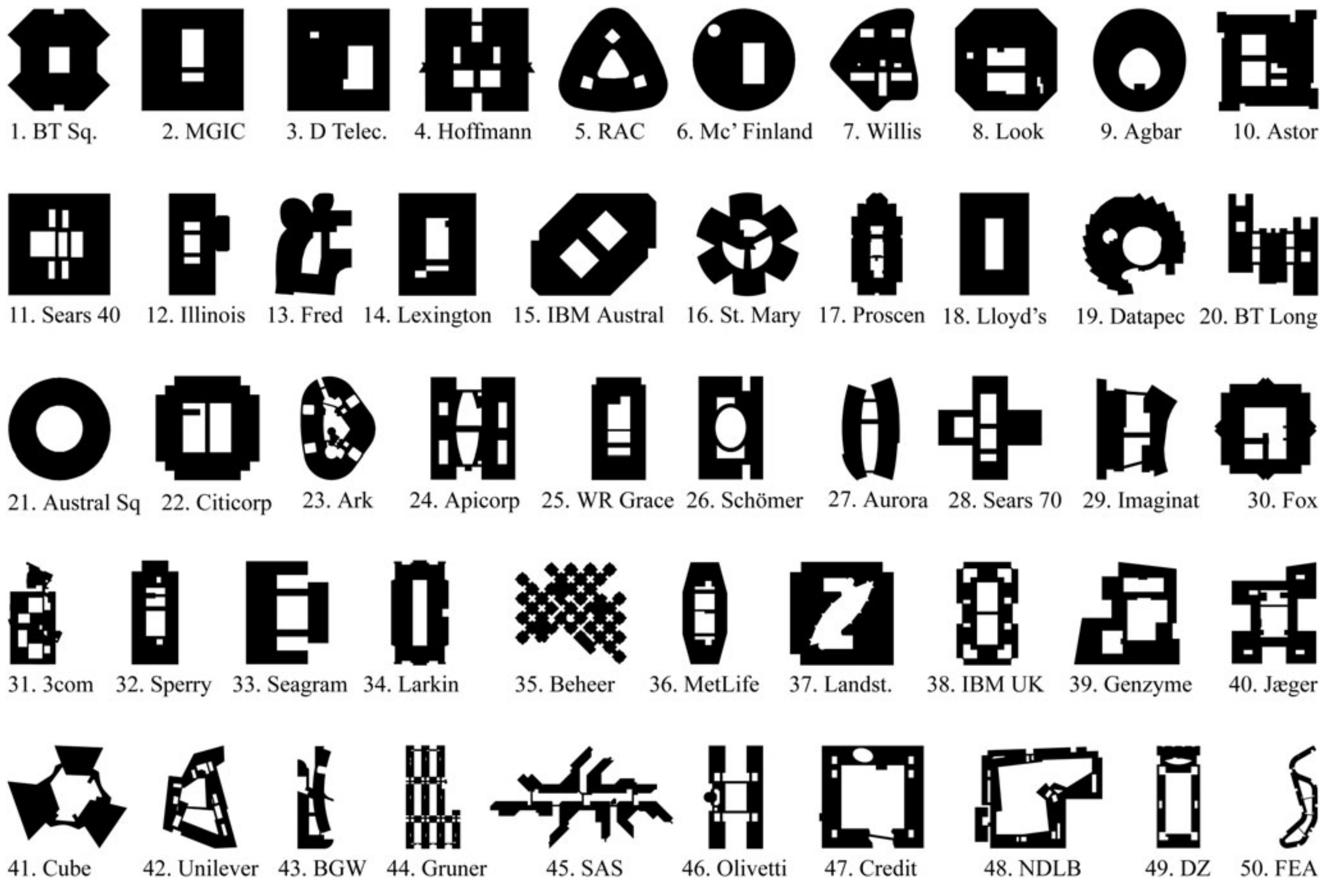

Fig. 7. The sample of 50 office floorplates with ring circulation listed according to ascending relative distance values.

4. DIRECTIONAL FRAGMENTATION (DF)

The second measure is DF. This is an index of the universal change of direction of travel between locations in a shape and corresponds to the kinetic inertia of movement. Directional changes are measured according to visibility graph distances (Turner et al., 2001). The index is normalized for size by dividing the aggregate distance by the shape area.

$$\mathrm{DF} = \frac{1}{n^2} \sum_{i=1,j=1}^{i=n,j=n} v_{ij}, \qquad (5)$$

where v_{ij} is the visual depth or directional distance between two units i and j, and n is the number of units in a shape (Fig. 1d and e). The visual depth between two co-visible points is established as 0; therefore, DF equals 0 for a convex shape. The index varies slightly when a shape is represented with different numbers of units; however, it stabilizes for fine representations. The index yields almost identical results between calculating with visibility depth and overlapping convex depth as demonstrated by the strong correlation ($r^2 = 0.926$) for a sample of 50 urban shapes (Shpuza, 2007). Fragmentation in shapes is achieved in two ways: by adding wings and increasing the jaggedness of the perimeter; by adding holes and increasing the size of holes in the shape.

For the purpose of this study, shapes are represented with fine meshes generally of 3000–8000 units, and with 29,000 units for a very complex shape such as Venice. The calculation of the two shape measures is carried out using the Java application *Qelizë*, which in its enhanced version supports the calculation of *RD* with both shortest path distance and taxicab distance, and *DF* with both visual depth and overlapping convex depth.

5. MORPHOSPACE OF COUPLED SHAPE MEASURES

A 2-D morphospace is proposed based on joint use of the developed measures of distance RD and directionality DF. Originating from studies in biology, the concept of morphospace has been used for the classification of built form based on topological characteristics of shape (Steadman & Mitchell, 2010). For the purpose of this study, the morphospace is defined according to the scatterplot between RD values of shape in the horizontal *x* axis, and DF values of shape in the vertical *y* axis. The morphospace bridges between two main disciplines of shape description. It conveys quantitative descriptions of two features of shape, thus belonging to morphome-

https://doi.org/10.1017/S0890060411000217 Published online by Cambridge University Press

Table 3. *Catalogue of the sample of 50 office floor plates with linear circulation listed according to ascending relative distance values*

Name	Floor	Architect	Location
1. DuPont	T	Unknown	Wilmington, DE, USA
2. IBM Regional	T	Unknown	Cranford, NJ, USA
3. Steelcase	T	WBDC, Inc.	Grand Rapids, MI, USA
4. Ford Motor	T	Unknown	Cologne, Germany
5. WMA Consulting Engineering	T	Unknown	Chicago, IL, USA
6. Menara Mesiniaga	6	Ken Yeang	Subang Jaya, Malaysia
7. Buch and Ton	T	Unknown	Güttersloh, Germany
8. Council House 2	T	Mick Pearce/Design	Melbourne, Australia
9. Albirr Foundation	15	Perkins & Will	Riyadh, Saudi Arabia
10. Sharp	T	Shimizu Corporation	Makuhari, Japan
11. 4 New York Plaza	T	Carson, Lundin & Shaw	New York, NY, USA
12. Lever House	T	Gordon Bunshaft, SOM	New York, NY, USA
13. Montgomery Ward	T	Minoru Yamasaki	Chicago, IL, USA
14. Weyerhaeuser	1	SOM	Tacoma, WA, USA
15. Lloyd's Register of Shipping	8	Richard Rogers Partnership	London, UK
16. McDonald's Italia	T	Atelier Mendini	Milan, Italy
17. Inland Steel	T	SOM	Chicago, IL, USA
18. Eastman Kodak	T	Unknown	Rochester, NY, USA
19. 88 Wood Street	10	Richard Rogers Partnership	London, UK
20. Interpolis	T	Abe Bonema	Tilburg, The Netherlands
21. Rockefeller Center	T	The Associated Architects	New York, NY, USA
22. Commerzbank	T	Sir N. Foster & Partners	Frankfurt, Germany
23. Pirelli Building	T	Ponti & Nervi	Milan, Italy
24. John Deere	T	Eero Saarinen & Associates	Moline, IL, USA
25. Channel 4 Television	T	Richard Rogers Partnership	London, UK
26. Deutsche Bundesstiftung Umwelt	T	E. Schneider-Wessling	Osnabrück, Germany
27. U-Building	T	Kazuyo Sejima & Ryue Nishizawa	Ushiku, Japan
28. Vitra International	2	F. Gehry & Assoc.	Basel, Switzerland
29. Campus MLC	2	Bligh Voller Nield	Sydney, Australia
30. Monsanto	T	Holey Assoc.	St. Louis, MO, USA
31. Arthur Andersen	T	Unknown	London, UK
32. Chiat/Day Advertising	2	F. Gehry & Assoc	Venice, CA, USA
33. Cellular Operations	1	Richard Hywel Evans	Swindon, UK
34. IBM Global	3	Kohn Pedersen Fox Assoc.	Armonk, NY, USA
35. Hypo Alpe-Adria Bank	6	Morphosis	Udine, Italy
36. Ford Foundation	T	Kevin Roche & John Dinkeloo	New York, NY, USA
37. Previsión Española	2	Rafael Moneo	Sevilla, Spain
38. Dutch Embassy	1	D. van Gameren, B. Mastenbroek	Addis Ababa, Ethiopia
39. Dooradoyle Civic Offices	2	Bucholz McEvoy	Dooradoyle, Ireland
40. LVA	3	Behnisch	Lübeck, Germany
41. Cerved	T	V. Moretti & C. Saratti	Padua, Italy
42. IBM Regional Center	T	Gwathmey, Siegel & Assoc.	Greensboro, NC, USA
43. Provinciehuis	T	Kohn Pedersen Fox	Hague, The Netherlands
44. Kildare Civic Offices	1	Heneghan Peng & A. Gibney	Kildare, Ireland
45. Hypolux Bank	4	Richard Meier	Luxembourg, Luxembourg
46. Banque Populaire O+A	1	O. Decq & B. Cornette	Rennes, France
47. Bayer Konzernzentrale	4	Murphy Jahn	Leverkusen, Germany
48. Burda Media Park	2	Ingenhoven Overdiek Kahlen	Offenburg, Germany
49. Stealth	2	Eric Owen Moss	Culver City, CA, USA
50. Reebok	3	NBBJ	Canton, MA, USA

try. At the same time, the combined state of the measures produce qualitative topological classifications of shape, and thus also belongs to morphology.

Each shape occupies a specific position according to RD and DF pairs. As a corollary, the study tests the hypothesis that the coupled measures represent a unique description of shape; that is, no two different shapes have the same pair of RD and DF values. The morphospace characterizes both topological and dimensional features of shape, given the definition of the two measures. Its dimensionality is fixed and minimal, requiring only two shape indices. From this conceptual viewpoint, it differs from methods that utilize large numbers of arbitrary shape attributes for formal classification of built forms (Hanna, 2010).

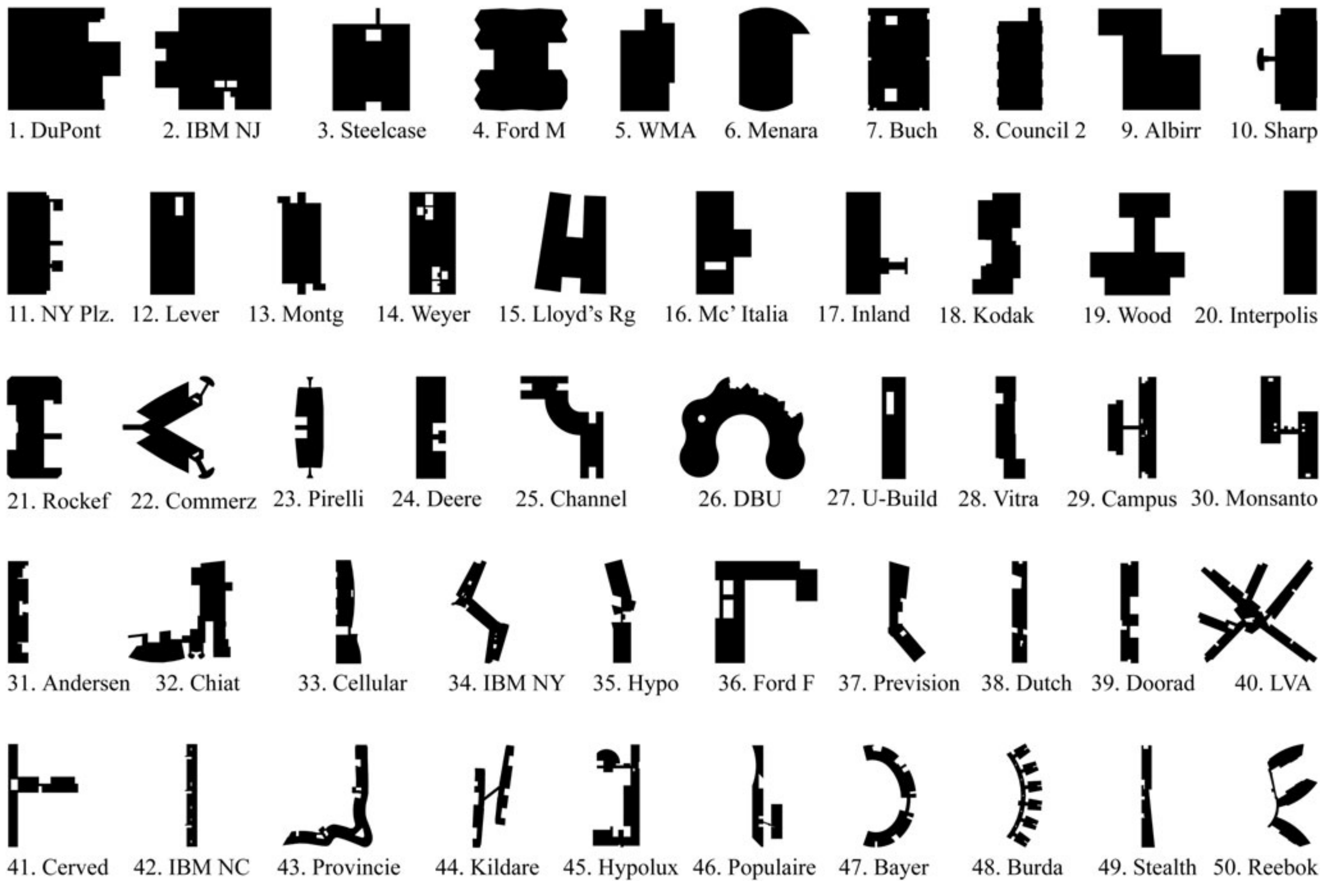

Fig. 8. The sample of 50 office floorplates with linear circulation listed according to ascending RD values.

The two proposed measures gauge distinct aspects of shape while showing a complex relationship with each other. On the one hand, an increase in shape fragmentation (i.e., higher DF) is always followed by a decrease in compactness (i.e., higher RD). The inverse of this relation is not possible; no fragmented shape can have the same compactness as the square, as illustrated by the lack of data points in the wedge region between the limit line and y axis (Fig. 2a). The definition of the equation of the line bounding the area of possible combinations of RD and DF is a mathematical problem *sui generis* that remains to be solved.

However, on the other hand, it is possible to endlessly elongate a convex shape, thus increasing its RD, while keeping a constant DF of 0, thus occupying positions in the lower area of the plot along the x axis. The asymmetrical relationship between the two measures explains in part the preference for the concept of compactness by most geographical studies in the past. At the same time, this discussion illustrates how one measure alone cannot suffice to fully describe the complexity of shape.

6. THEORETICAL SHAPES

Boundary shapes of polyomino arrangements (Golomb, 1996) are analyzed for the purpose of understanding the potential covariance between the two measures. Starting with an elementary square tile, the increase of number of tiles, or polyomino order, produces combinations of contiguous shapes that can represent any actual shape. Polyomino families ($n = 1$ to 6; Fig. 3) are shown in morphospace with lines connecting data points ranked according to RD values (Fig. 2a). The higher order polyominoes include increasingly complex shapes. Although their family lines become progressively more jagged, they maintain an overall inverted "U" contour and offset incrementally up and toward the right, thus filling the area to the right of the limit line. However, most data points in each family are located along the left half of the inverted "U" lines, spanning between the origin and the apex; considered separately, these cases show high positive correlations between the two measures. This leads to the speculation that although it is possible to produce shapes that can occupy any position to the right of the limit lines in morphospace, most shapes occupy a narrower region with a positive correlation between the two measures starting at the (RD = 1, DF = 0) origin and extending toward the upper right.

The further increase of polyomino order generates shapes that contain holes. A second sample of theoretical shapes is constructed as a subset of 4655 decominoes ($n = 10$) containing all 16 instances with topological disc holes (Myers, 2010),

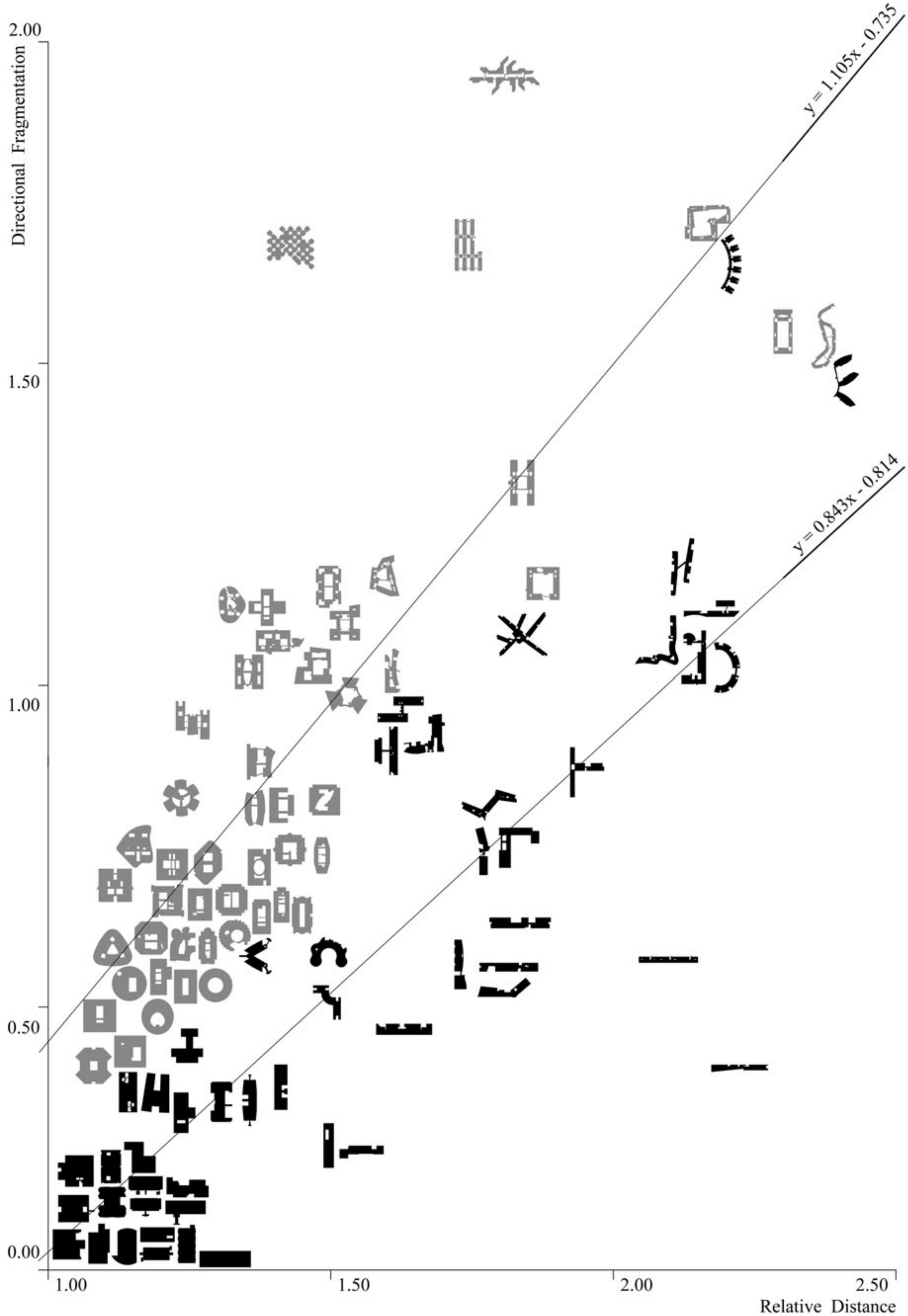

Fig. 9. Fifty ring office floorplates (gray) and 50 linear office floorplates (black) compared according to relative distance and directional fragmentation.

https://doi.org/10.1017/S0890060411000217 Published online by Cambridge University Press

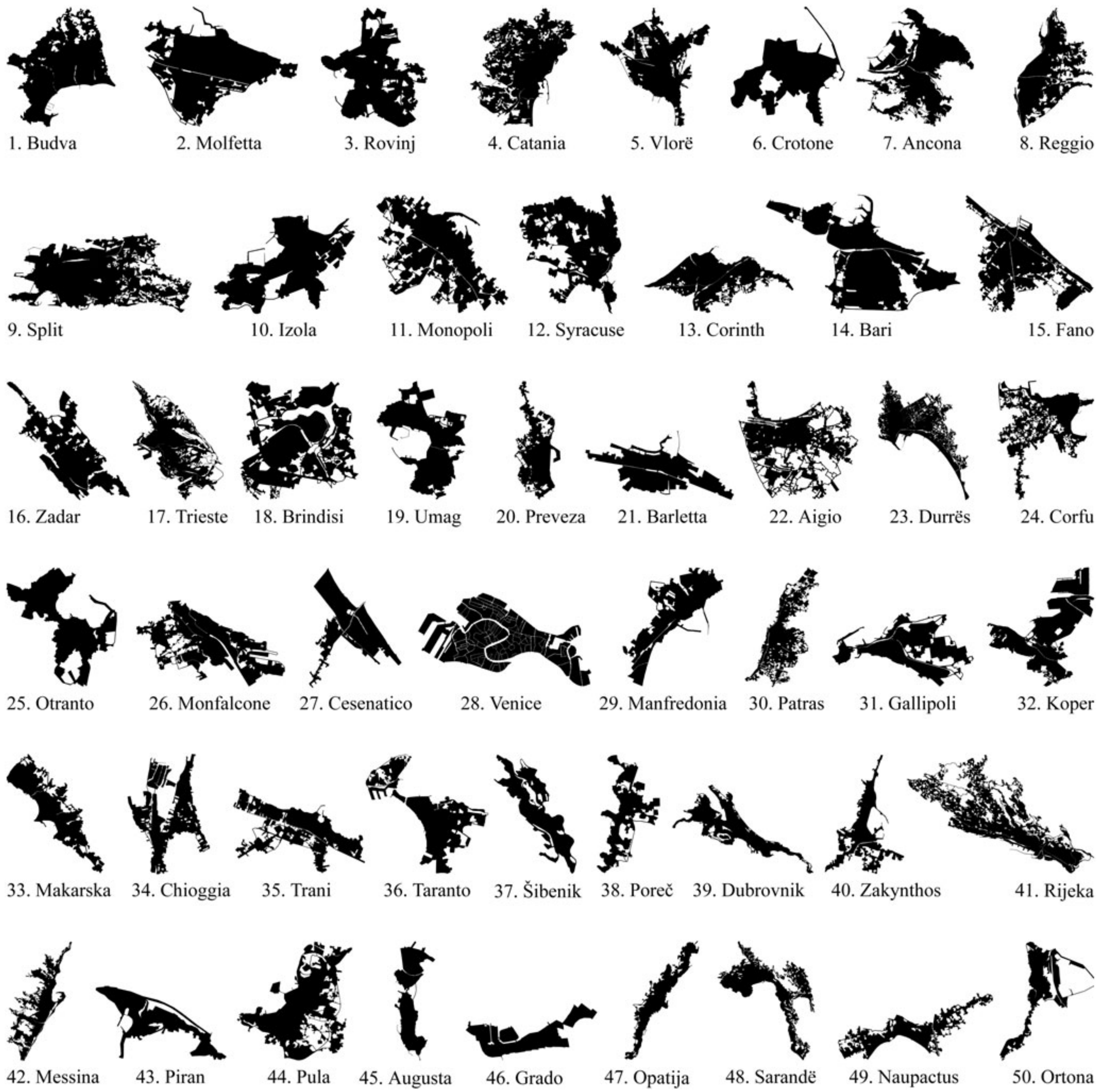

Fig. 10. The sample of 50 urban shapes of Adriatic and Ionian coastal cities listed according to ascending shape hull relative distance values.

16 cases randomly selected from 179 decominoes with nontopological holes, and 16 cases from compact shapes. The location of data points in the scatterplot reinforces the above trend with regard to the inverted "U" scatter and the accumulation of most data points along the left half of the crescent (Fig. 2b). Shapes with topological disc holes occupy a specific area in morphospace along the upper extremity of the scatter, the nontopological holes have a wider spread while maintaining a linear scatter, whereas the solid shapes fall across the entire span of the crescent. This raises the possibility that, when compared to solid shapes, shapes with holes represent distinct correlations between RD and DF. Theoretically possible correlations between the two measures are likely to have different specific actualizations in boundary shapes of various types of built form.

Mazes are another class of theoretical shapes that are generated by arranging square tiles according to compositional rules of a topological nature. Here, the boundary shapes of mazes are analyzed in order to understand the effect of underlying generative principles on the relationship between compactness and fragmentation of shape. Four kinds of mazes—*braid*, *cavern*, *crack* and *perfect*—are considered as examples of different rules concerning dead-ends, loops, junctions, in-

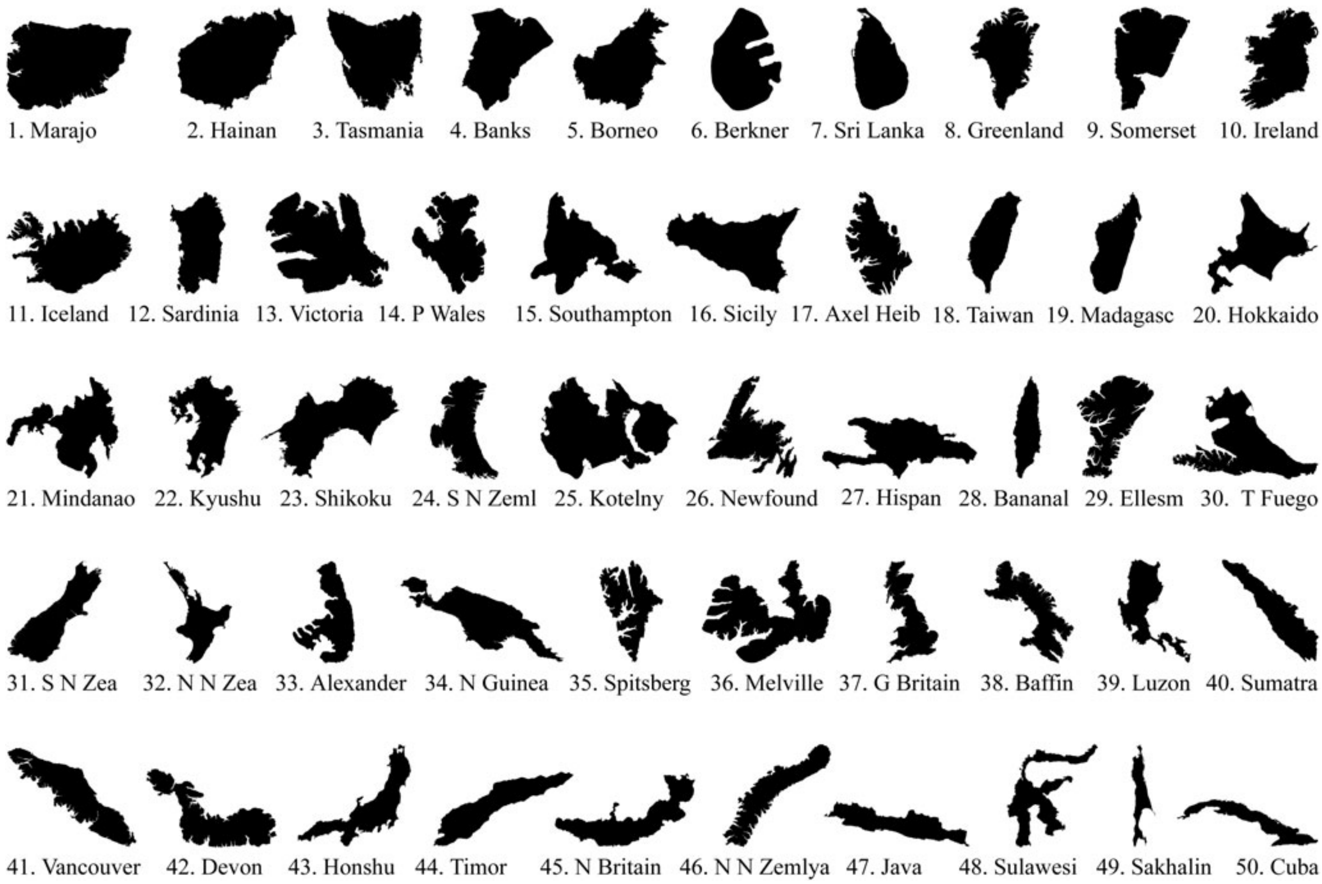

Fig. 11. The shapes of the 50 largest islands in the world listed according to ascending relative distance values.

accessible areas, walls, and passages. They are generated using *Daedalus* software (Pullen, 2011) in four series, including five shape groups of 3×3, 4×4, 5×5, and 6×6 sizes, totaling 80 cases (Fig. 4).

For each series, shape groups are shown in morphospace with lines connecting data points ranked according to RD (Fig. 5). The increase of DF indicates higher maze complexity. The relative positioning of the four-maze series in morphospace illustrates that complexity increases from crack to cavern, to braid, to perfect. In addition, the increase of maze size leads to more complex shapes as indicated by the higher location of incremental size groups in the plot. In crack mazes, the offset among groups is smaller and confined to comparable RD values, thus indicating small increase of complexity due to size increase, and that complexity is achieved while maintaining rather stable compactness. In contrast, size increase in perfect mazes leads to a rapid increase in complexity that is equally matched by increased elongation of shape. Considered together, the 80 mazes show a strong and significant correlation ($r = 0.843$, $p < 0.001$). Unlike polyominoes, the morphogenetic rules in mazes are manifested in a close relationship between RD and DF of boundary shapes. This raises the premise that various types in the built environment occupy distinct regions of morphospace with specific correlations between compactness and fragmentation.

7. ACTUAL BOUNDARY SHAPE CLASSES

Six samples of boundary shapes from various classes in the built environment and physical geography are analyzed with the twofold purpose of understanding their position in the proposed morphospace and inquiring into the effect of underlying circulation structures on boundary shape conditions.

Houses are a built type with elementary circulation, in both topological and metric terms, that links rooms and open plan components. The requirement for easy access between spaces often leads to compact forms. A sample of 50 detached houses is selected based on 20th century design masterpieces (Davies, 2006; Table 1, Fig. 6). House floorplates are analyzed according to RD and DF. The plot between the two measures shows a weak correlation, suggesting that elementary circulation systems are associated with a wide range of conditions of boundary shapes that lack a clear relationship between compactness and fragmentation (Fig. 13a).

Office buildings represent a built type with a close relationship between main circulation and floorplate geometry (Shpuza, 2006; Shpuza & Peponis, 2008). Office floorplates

https://doi.org/10.1017/S0890060411000217 Published online by Cambridge University Press

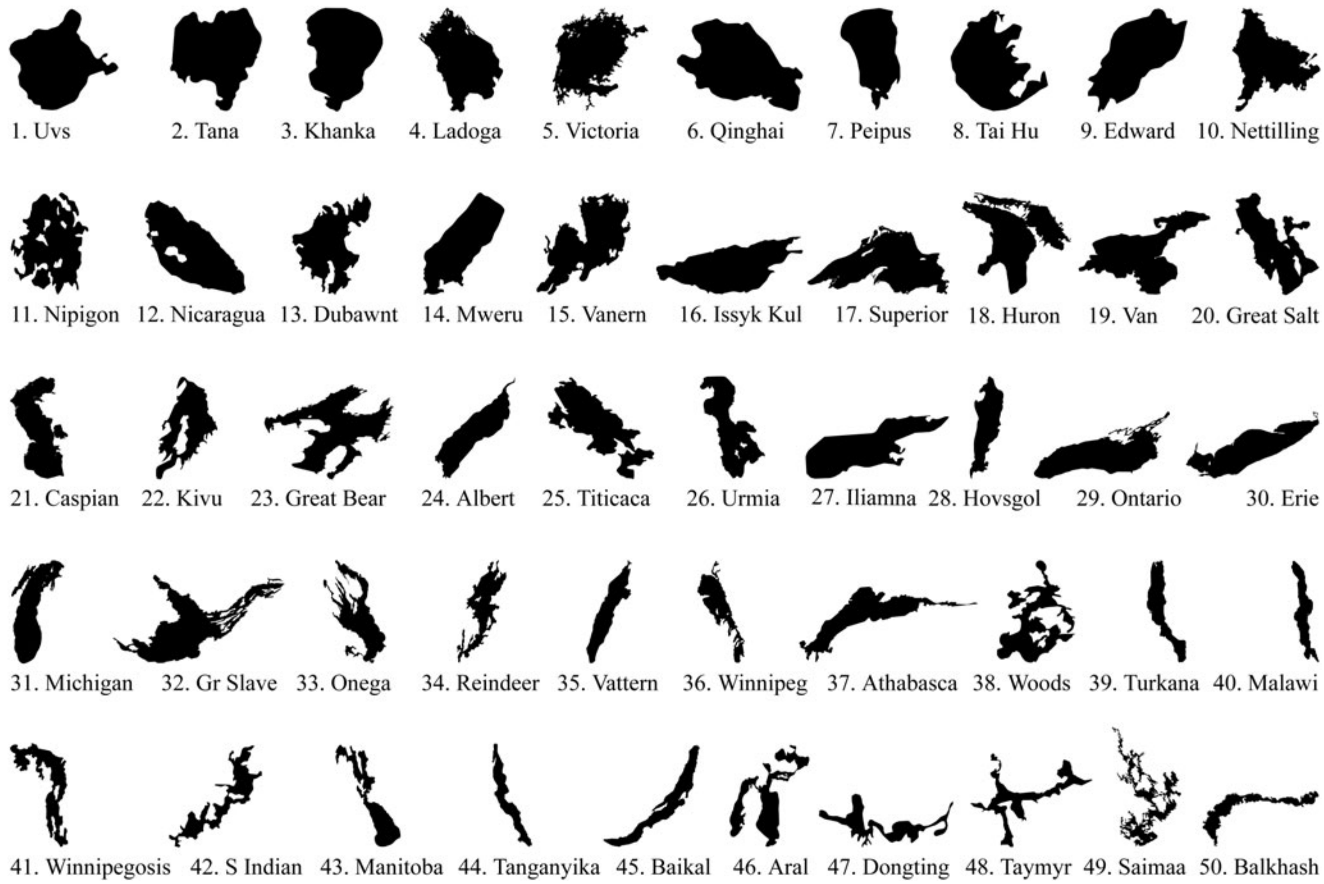

Fig. 12. The shapes of the 50 largest stable lakes in the world listed according to ascending relative distance values.

are, to some degree, offset projections of the main circulation system given specific depths of leasing space and rooms (differences between open plan and cellular configurations not withstanding). It is thus to be expected that office floorplates exhibit strong typological features that position them in distinct areas of morphospace. This study recognizes two fundamental categories of main circulation in offices: ring and linear. Ring circulation systems are those where there exists at least a second alternative path between two positions along the main circulation system. By contrast, linear circulation systems offer only one path between such locations. A subsample of 50 ring office buildings (Table 2, Fig. 7; Pile, 1976; Bedarida & Milatović, 1991; Duffy & Powell, 1997; Myerson & Ross, 1999; Various authors, 2004–2009; Hascher et al., 2002; Shpuza, 2006; Gregory, 2008; van Meel, 2010; Weston, 2010) and a subsample of 50 linear office buildings (Table 3, Fig. 8; Pile, 1976; Duffy & Powell, 1997; Bedarida & Milatović, 1991; Myerson & Ross, 1999; Albrecht & Broikos, 2000; van Meel, 2000; Hascher et al., 2002; Blaser, 2003; Shpuza, 2006; Futagawa, 2008; Gregory, 2008; Weston, 2010) was selected based on best practice examples of office buildings from 1904 to the present. There exist strong and significant correlations between RD and DF for both ring office floorplates ($r = 0.811$) and linear ones ($r = 0.846$). However, the correlation decreases ($r = 0.674$) when the two subsamples (100 cases) are analyzed together. The data points from each subsample occupy separate regions in morphospace as illustrated by the marginal overlap between them (Fig. 9). The linear regressions of the two subsamples exhibit a significant inequality (Zar, 2009), thus confirming that the two categories of office buildings constitute different ways of correlating compactness and fragmentation. Ring offices show a greater variety of shape fragmentation, whereas linear offices show a greater variety of shape compactness. Topological differences between the two kinds of underlying main circulation systems are therefore materialized in striking morphological disparities between two classes of floorplate shape.

Urban shapes are generated upon circulation structures of street networks according to the process of filling urban blocks. Street networks are complex systems with high degree of connectivity and choice. A sample of 50 urban shapes was selected from the Adriatic and Ionian littoral zones (Google Earth, 2006–2010). It includes some of the largest populated centers and a few towns of historical significance on the Italian coast, and 25 urban centers with populations greater than 10,000 on the coast of Slovenia, Croatia, Montenegro, Albania, and Greece. These cities display a wide diversity of urban shapes affected by various physiographic conditions of bays, lagoons, deltas, islands, promontories, and narrow strips of land bound by the shoreline and hilly terrains

https://doi.org/10.1017/S0890060411000217 Published online by Cambridge University Press

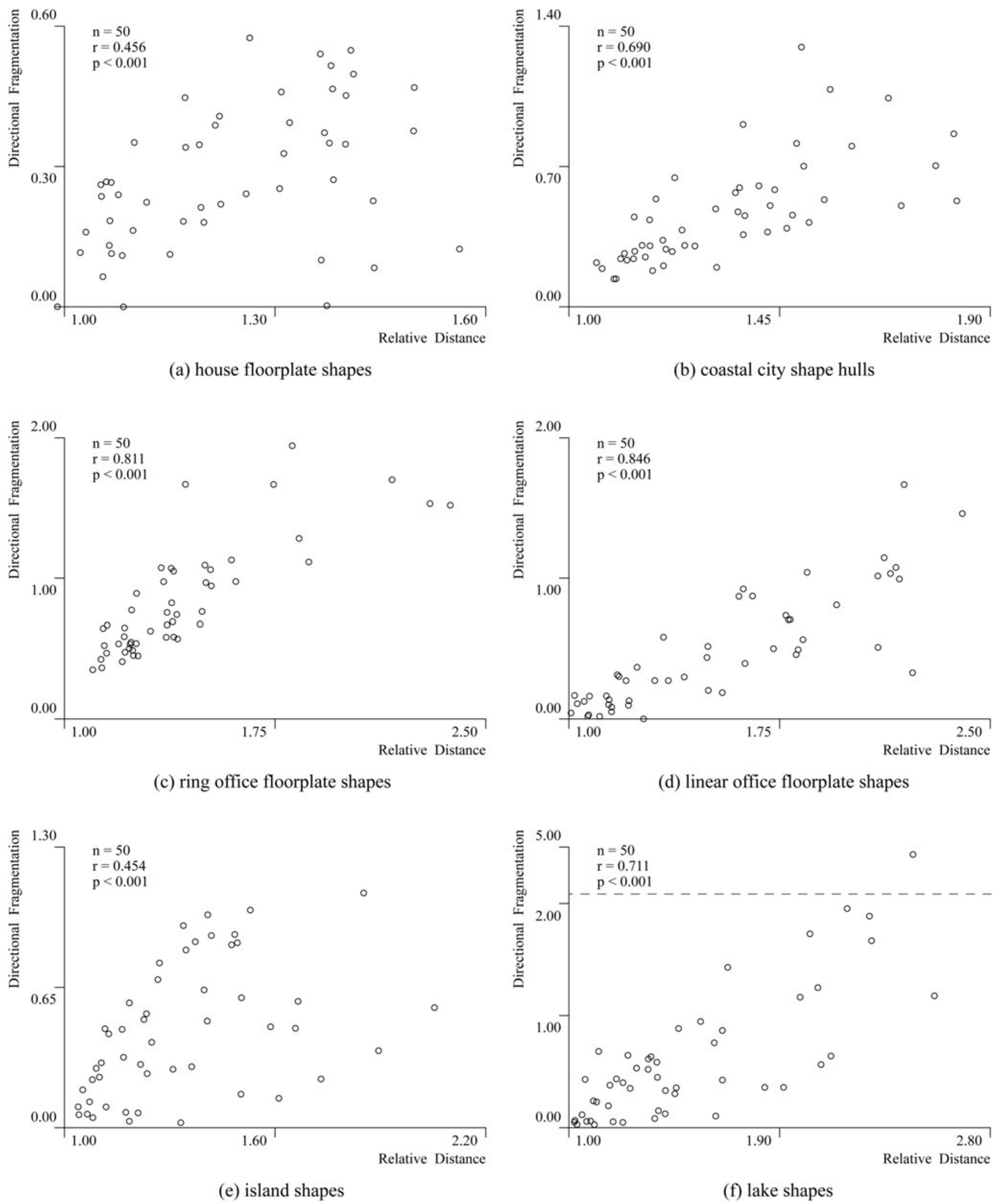

Fig. 13. Scatterplots between relative distance and directional fragmentation for six classes of boundary shape.

https://doi.org/10.1017/S0890060411000217 Published online by Cambridge University Press

(Fig. 10). The analysis of actual urban shapes shows a weak and insignificant ($r = 0.225$) covariance between the two indices. However, when urban shape hulls are analyzed (i.e., holes in the urban shapes are ignored), a strong and significant ($r = 0.690$) correlation emerges (Fig. 13b). This indicates that urban forms internalize the effect of holes to exert a strong balance between compactness and fragmentation and overcome apparently insurmountable obstacles of the terrain.

Two samples of boundary shape from physical nature are analyzed for the purpose of inquiring into the relationship between RD and DF. One includes the shapes of the 50 largest islands in the world (Fig. 11), and the other includes the shapes of world's 50 largest lakes with stable water levels (Fig. 12). Island and lake shapes are obtained from the Natural Earth (2010) database using conformal WGS 1984 projections according to specific UTM zones. Despite a seemingly wide variety of shapes that lack human order, the two samples combined reveal ambivalent relationships between the two measures. Although island shapes show a weak correlation between RD and DF (Fig. 13e), lake shapes show a strong and significant correlation ($r = 0.711$; Fig. 13f). The correlation for lake shapes improves further ($r = 0.764$) if the outlier, Lake Saimaa, is excluded. The explanation of this discrepancy between island and lake shapes, if indicative of any geophysical phenomenon, falls to the domain of physiographic studies. For this argument, of interest the fact that correlations between RD and DF are not limited to types in the built environment, but also include classes in nature.

The morphospace constructed according to the two measures is used for the comparative study of form. Each class from the built environment and nature is represented with a polygon that is drawn according to the convex hull of data points in the scatterplot (Fig. 14). In general, class polygons are positioned in the zone with a positive correlation between

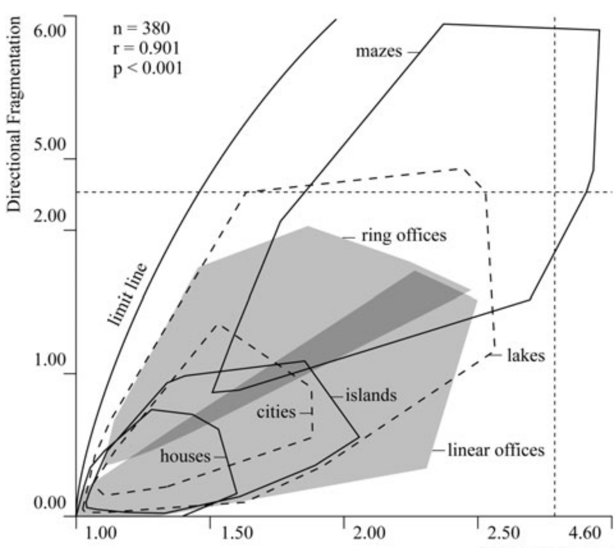

Fig. 14. The position of boundary shape classes in morphospace.

RD and DF, just to the right of the limit line thus illustrating an overall balance between distance and directionality for actual shapes. The correlation between RD and DF for 300 combined actual shapes of houses, cities, offices, islands, and lakes is $r = 0.679$ ($p < 0.001$), and for 380 cases including mazes is $r = 0.901$ ($p < 0.001$). No class extends to the wedge region on the lower right alongside the *x* axis, which would include extremely elongated convex shapes. Houses are positioned in the lower left corner of the morphospace and include compact and simple floorplate shapes. The small extent of this polygon denotes little variance among house shapes. Urban shape hulls are positioned further above along the *y* axis. Two subsamples of office buildings, shown in gray, extend further on both directions to include a wide range of forms that are still bound inside distinct wedgelike regions. Mazes are positioned up and to the right and include the most complex shapes. Lakes include a wider variety of shapes than islands as indicated by the extent of the polygon high and to the right in the morphospace.

8. DISCUSSION

This study contributes a configurational approach situated within the discipline of space syntax for analyzing shape based on two elemental experiences of moving through space: covering distances and changing direction of travel. Boundary shapes are considered according to a balanced diagram of forces, of which the internal forces exerted by circulation systems in buildings and street networks in cities is given priority. The study is developed on the premise that the dialogue between centrality and visibility (Hillier, 1996) in circulation systems and street networks affects boundary shapes to maintain a close relationship between compactness and fragmentation and manifest features of emergence and dynamic order in the built form (Hillier et al., 1993; Hillier, 1999). The proposed method of describing shape takes into account dimensional aspects of form and weighs the configurational analysis with metrics. It contributes normalized shape indices that do not depend on the number of representational units. In contrast to measures of shape based on the description of perimeter, here a space to shape approach is used whereby conditions or each location in space contribute to the shape description.

This paper suggests important implications for the study of form. First, the simultaneous description of shape according to RD and DF suggests a "unique" approach to shape description. The empirical analysis of 484 shapes in eight samples shows that no two shapes have the same pair of values for RD and DF. The claim remains to be tested further with empirical studies of larger data sets of shapes.

Second, it is shown that actual boundary shapes of various classes in the built environment occupy distinct regions in morphospace and utilize a specific portion of combinations that are theoretically possible.

Third, from the viewpoint of the interaction between boundary shape and embedded circulation, it is suggested that specific conditions of shape for various classes are mediated by

https://doi.org/10.1017/S0890060411000217 Published online by Cambridge University Press

the configuration of the underlying main circulation. Elementary circulation systems, such as for detached houses, show weak correlations between compactness and fragmentation of floorplate shapes. In contrast, developed circulation systems in offices and cities are matched by strong correlations between distance and directionality of floorplate shapes and urban shapes. Furthermore, configurational disparities between ring and linear circulation systems in office buildings are manifested in distinct classes of floorplate shapes that occupy separate regions in morphospace. This economy of balancing various degrees of distance and directionality points to the application of "principles of least action" (Mayer, 1877) underlying the generation of man-made boundaries.

The study contributes unique descriptive measures of shape, a morphospace of coupled shape measures, and a comparative approach to the study of built environment and nature. The paper raises theoretical implications for understanding the intricate relationship between boundary and circulation in the built environment and for supporting experimental and generative algorithms in aid of design and planning.

ACKNOWLEDGMENTS

The author thanks Sean Hanna and the anonymous reviewers for their constructive recommendations, John Peponis for the criticism that led to a wider scope of argumentation for the study, Martin Scoppa, who facilitated the projection of geographical shape files, and Fisnik Shpuza, who generously programmed the latest version of Qelizë.

REFERENCES

Albrecht, D., & Broikos, C. (2000). *On the Job: Design and the American Office*. New York: Princeton University Press and Washington, DC: National Building Museum.

Alexander, C. (1964). *Notes on the Synthesis of Form*. Cambridge, MA: Harvard University Press.

Austin, R.F. (1984). Measuring and comparing two-dimensional shapes. In *Spatial Statistics and Models* (Gaile, G.M., & Willmott, C.J., Eds.), pp. 293–312. Boston: D. Reidel.

Batty, M. (2001). Exploring isovist fields: space and shape in architectural and urban morphology. *Environment and Planning (B): Planning and Design 28*, 123–150.

Bedarida, M., & Milatović, M. (1991). *Bürogebäude*. Stuttgart: Karl Krämer.

Blair, D.J., & Biss, T.A. (1967). Measurement of shape in geography: an appraisal of methods and techniques. In *Bulletin of Quantitative Data for Geographers 11*, Nottingham: Nottingham University, Department of Geography.

Blaser, W. (2003). *Bayer Konzernzentrale Headquarters*. Basel: Birkhäuser.

Bunge, W. (1966). *Theoretical Geography*. Lund: C.W.K. Gleerup.

Clark, W.A.V., & Gaile, G.L. (1973). The analysis and recognition of shapes. *Geografiska Annaler. Series B, Human Geography 55(1)*, 153–163.

Conroy, R. (2001). *Spatial navigation in immersive virtual environments*. PhD Thesis, University College London.

Cooke, C. (1975). Nikolai Krasil'nikov's quantitative approach to architectural design: an early example. *Environment and Planning B: Planning and Design 2*, 3–20.

Davies, C. (2006). *Key Houses of the Twentieth Century: Plans, Sections and Elevations*. New York: Norton.

Duffy, F. (1974). Office design and organizations: 1. Theoretical basis. *Environment and Planning B: Planning and Design 1*, 105–118.

Duffy, F., & Powell, K. (1997). *The New Office*. London: Conrad Octopus.

Futagawa, Y. (2008). *GA Contemporary Architecture, Office 2*, 11. Tokyo: ADA Edita.

Gibson, J.J. (1979). *The Ecological Approach to Visual Perception*. Boston: Houghton Mifflin.

Golomb, S. (1996). *Polyominoes: Puzzles, Patterns, Problems and Packings*. Princeton, NJ: Princeton University Press.

Google Earth. (2006–2010). Retrieved April 2006–August 2010.

Gregory, R. (2008). *Key Contemporary Buildings: Plans, Sections and Elevations*. New York: Norton.

Haggett, P., & Chorley, R.J. (1969). *Network Analysis in Geography*. London: Edward Arnold.

Hanna, S. (2010). Design agents and the need for high-dimensional perception. In *Design Computing and Cognition '10* (Gero, J.S., Ed.), pp. 115–134. Stuttgart: Springer.

Hascher, R., Jeska, S., & Klauck, B. (2002). *Office Buildings: A Design Manual*. Basel: Birkhäuser.

Hillier, B. (1996). *Space is the Machine*. Cambridge: Cambridge University Press.

Hillier, B. (1999). The hidden geometry of deformed grids: or, why space syntax works when it looks as though it shouldn't. *Environment and Planning B: Planning and Design 26*, 169–191.

Hillier, B., & Hanson, J. (1989). *The Social Logic of Space*. Cambridge: Cambridge University Press.

Hillier, B., Penn, A., Hanson, J., Grajewski, T., & Xu, J. (1993). Natural movement: or, configuration and attraction in urban pedestrian movement. *Environment and Planning (B): Planning and Design 20*, 29–66.

Koenderink, J.J. (1990). *Solid Shape*. Cambridge, MA: MIT Press

Maceachren, A. (1985). Compactness of geographic shape: comparison and evaluation of measures. *Geografiska Annaler. Series B, Human Geography 67(1)*, 53–67.

March, L., & Steadman, P. (1971). *The Geometry of Environment*. London: RIBA Publications.

Mayer, A. (1877). *Geschichte des Prinzips der Kleinsten Action*. Leipzig: Veit.

Moellering, H., & Rayner, J. (1981). The harmonic analysis of spatial shapes using dual axis fourier shape analysis (DAFSA). *Geographical Analysis 13(1)*, 64–77.

Myers, J. (2010). *Polyomino tiling*. Accessed at http://www.srcf.ucam.org/~jsm28/tiling/

Myerson, J., & Ross, P. (1999). *The Creative Office*. Corte Madera, CA: Gingko Press.

Natural Earth. (2010). *1:110m Physical vectors.* Accessed at http://www.naturalearthdata.com/downloads/110m-physical-vectors on September 2010.

Peponis, J., & Wineman, J. (2002). Spatial structure of environment and behavior. In *Handbook of Environmental Psychology* (Bechtel, R.B., & Churchman, A., Eds.), pp. 271–291. New York: Wiley.

Peponis, J., Wineman, J., Rashid, M., Hong Kim, S., & Bafna, S. (1997). On the description of shape and spatial configuration inside buildings: convex partitions and their local properties. *Environment and Planning B: Planning and Design 24*, 761–781.

Piaget, J., & Inhelder, B. (1967). *The Child's Conception of Space*. London: Routledge & Kegan Paul.

Pile, J. (1976). *Interior 3rd Book of Offices*. New York: Watson–Guptill.

Psarra, S., & Grajewski, T. (2001). Describing shape and shape complexity using local properties. *Proc. 3rd Int. Symp. Space Syntax*, pp. 28.1–28.6.

Pullen, W.D. (2011). *Daedalus 2.3*. Available at http://www.astrolog.org/labyrnth/daedalus.htm on February 2011.

Shpuza, E. (2001). Floorplate shapes as generators of circulation. *Proc. 3rd Int. Symp. Space Syntax*, pp. 29.1–29.15.

Shpuza, E. (2006). *Floorplate shapes and office layouts: a model of the effect of floorplate shape on circulation integration.* PhD Dissertation, Georgia Institute of Technology. Accessed at http://etd.gatech.edu/theses/available/etd-03172006-111654

Shpuza, E. (2007). Urban shapes and urban grids: a comparative study of Adriatic and Ionian coastal cities. *Proc. 6th Int. Space Syntax Symp.*, pp. 9.01–9.25.

Shpuza, E., & Peponis, J. (2008). The effect of floorplate shape upon office layout integration. *Environment and Planning B: Planning and Design 35(2)*, 318–336.

Steadman, P. (2003). How day-lighting constrains access. *Proc. 4th Int. Symp. Space Syntax*, pp. 5.1–5.18.

Steadman, P., & Mitchell, L.J. (2010). Architectural morphospace: mapping worlds of built forms. *Environment and Planning B: Planning and Design 37(2)*, 197–220.

Tabor, P. (1976). Analyzing route patterns. In *The Architecture of Form* (March, L., Ed.), pp. 352–378. Cambridge: Cambridge University Press.

Taylor, P. (1971). Distances within shapes: an introduction to a family of finite frequency distributions. *Geografiska Annaler. Series B, Human Geography 53(1)*, 40–53.

Thompson, D.W. (1959). *On Growth and Form*. Cambridge: Cambridge University Press.

Turner, A., Doxa, M., O'Sullivan, D., & Penn, A. (2001). From isovist to visibility graphs: a methodology for the analysis of architectural space. *Environment and Planning B: Planning and Design 28*, 103–122.

van Meel, J. (2000). *The European Office: Office Design and National Context*. Rotterdam: 010 Publishers.

Various Authors. (2004–2009). *Architectural Review, May 2004–Dec 2009*. London: Architectural Press.

Wentz, E. (2000). A shape definition for geographic applications based on edge, elongation and perforation. *Geographical Analysis 32(1)*, 95–112.

Weston, R. (2010). *Key Buildings of the 20th Century: Plans, Sections and Elevation*, 2nd ed. New York: Norton.

Willoughby, T.M. (1975). Building forms and circulation patterns. *Environment and Planning B: Planning and Design 2*, 59–87.

Zamani, P. (2008). *Views across boundaries and groupings across categories: the morphology of display in the galleries of the high museum of art 1983–2003*. PhD Dissertation, Georgia Institute of Technology.

Zar, J. (2009). *Biostatistical Analysis*. Upper Saddle River, NJ: Prentice Hall.

Ermal Shpuza is an Associate Professor of architecture at Southern Polytechnic State University. He teaches architectural and urban design studios and courses on spatial morphology, urban design theory, and environmental technology. He is a registered architect with many years of practice experience. His research interests span architectural and urban morphology, workplace environments, Mediterranean post-industrial urban history, and design computing.

https://doi.org/10.1017/S0890060411000217 Published online by Cambridge University Press